

The Hubble Constant from the HST Key Project on the Extragalactic Distance Scale

Laura Ferrarese¹, Brad K. Gibson², Daniel D. Kelson³, Shoko Sakai⁴,
 Jeremy R. Mould⁵, Wendy L. Freedman⁶, Robert C. Kennicutt, Jr.⁷,
 Holland C. Ford⁸, John A. Graham³, John Huchra⁹, Shaun M.
 Hughes¹⁰, Garth D. Illingworth¹¹, Lucas Macri⁹, Barry F. Madore¹²,
 Kim Sebo⁵, N.A. Silbermann¹² & Peter B. Stetson¹³

Abstract. The final efforts of the HST Key Project on the Extragalactic Distance Scale are presented. Four distance indicators, the Surface Brightness Fluctuation method, the Fundamental Plane for early-type galaxies, the Tully-Fisher relation and the Type Ia Supernovae, are calibrated using Cepheid distances to galaxies within 25 Mpc. The calibration is then applied to distant samples reaching $cz \sim 10000 \text{ km s}^{-1}$ and (in the case of SNIa) beyond. By combining the constraints imposed on the Hubble constant by the four distance indicators, we obtain $H_0 = 71 \pm 6 \text{ km s}^{-1} \text{ Mpc}^{-1}$.

1. Introduction

Back in 1984, the goal of the HST Key Project on the Extragalactic Distance Scale (hereafter, KP) was announced to be the measurement of the Hubble constant, H_0 , with 10% accuracy. The plan of attack was to set the zero points for a variety of secondary distance indicators by measuring distances to 18 nearby calibrators using the most reliable of the primary standard candles, Cepheid variables (Figure 1). Crucial to the success of the mission was the ability of secondary distance indicators to reach beyond the local supercluster into the unperturbed Hubble flow. Fifteen years later, four have proven up to the challenge: the Surface Brightness Fluctuation Method, the Fundamental Plane for early-type galaxies, the Tully-Fisher relation and the Type Ia Supernovae. All are subject to biases arising from implicit assumptions made on the stellar pop-

¹Hubble Fellow, California Institute of Technology, Pasadena CA 91125, USA; ²CASA, University of Colorado, Boulder, CO, USA; ³Department of Terrestrial Magnetism, Carnegie Institution of Washington, Washington DC 20015, USA; ⁴Kitt Peak National Observatory, NOAO, Tucson AZ 85726, USA; ⁵Research School of Astronomy & Astrophysics, Institute of Advanced Studies, ANU, ACT 2611, Australia; ⁶Carnegie Observatories, Pasadena CA 91101, USA; ⁷Steward Observatory, The University of Arizona, Tucson AZ 85721, USA; ⁸Johns Hopkins University and Space Telescope Science Institute, Baltimore MD 21218, USA; ⁹Harvard Smithsonian Center for Astrophysics, Cambridge MA 02138 USA; ¹⁰Royal Greenwich Observatory, Cambridge CB3 0HA, UK; ¹¹Lick Observatory, University of California, Santa Cruz CA 95064 USA; ¹²NASA/IPAC Extragalactic Database and California Institute of Technology, Pasadena CA 91125, USA; ¹³Dominion Astrophysical Observatory, Victoria, British Columbia V8X 4M6, Canada

ulation of the galaxies they target. Such biases, which could have serious effects if any one distance indicator were to be used alone, are attenuated when the constraints imposed by all indicators are combined. The final KP results are presented in Ferrarese et al. (2000a), Kelson et al. (2000), Sakai et al. (2000), Gibson et al. (2000), Mould et al. (2000) and Freedman et al. (2000). Here we will summarize those efforts, focusing on the merit and disadvantages of each indicators, and pointing out areas where future work is needed.

The following sets the scene for the remainder of this paper: the calibration of the PL relation is based on the LMC sample of Madore & Freedman (1991). It assumes a true distance modulus to the LMC of 18.50 ± 0.13 mag (Mould et al. 2000), no dependence of the Cepheid PL relation on the metallicity of the variable stars, a ratio of total to selective absorption $R_V = A(V)/E(B - V) = 3.3$, and a reddening law following Cardelli, Clayton and Mathis (1989). Each of these assumptions is examined and their effects on the final error budget are assessed in the last section. We strove for homogeneity between the Cepheid distance scale and all secondary distance indicators: the treatment of the calibrator sample is consistent internally and with the distant sample to which the calibration is applied (Ferrarese et al. 2000b, Macri et al. 2000, Gibson et al. 2000, Kelson et al. 2000), providing a meaningful comparison of the results. This is perhaps the most distinctive mark of the KP compared to previous work.

Table 1. Cepheid Calibrators for the Secondary Distance Scale

Galaxy	m-M (mag) ^a	Group/Cluster ^b	SBF ^c	FP ^c	TF ^c	SN Ia ^c	Reference ^d
N224	24.44±0.10	Local Group	•		•		Madore & Freedman 1991
N598	24.64±0.09	Local Group			•		Freedman et al. 1991
N925	29.84±0.08	N1023 Group			•		Silbermann et al. 1996
N1326A	31.43±0.07	Fornax Cluster		•			Prosser et al. 1999
N1365	31.39±0.10	Fornax Cluster		•	•		Silbermann et al. 1999
N1425	31.81±0.06	Fornax Cluster		•	•		Mould et al. 1999
N2090	30.45±0.08	N1808 Group			•		Phelps et al. 1998
N2541	30.47±0.08	N2841 Group			•		Ferrarese et al. 1998
N2403	27.51±0.24	M81 region			•		Madore & Freedman 1991
N3031	27.80±0.08	M81 Group	•		•		Freedman et al. 1994
N3198	30.80±0.06	N3184 Group			•		Kelson et al. 1999
N3319	30.78±0.10	N3184 Group			•		Sakai et al. 1999
N3351	30.01±0.08	Leo I Group		•	•		Graham et al. 1997
N3368	30.20±0.10	Leo I Group	•	•	•	•	Gibson et al. 2000
N3627	30.06±0.17	Leo region			•	•	Gibson et al. 2000
N3621	29.13±0.11	Isolated			•		Rawson et al. 1997
N4414	31.41±0.10	Coma Clouds			•	○	Turner et al. 1998
N4725	30.57±0.08	Coma Clouds	•		•		Gibson et al. 1998
IC4182	28.36±0.08	Coma Clouds region				•	Gibson et al. 2000
N4321	31.04±0.09	Virgo–M87		•			Ferrarese et al. 1996
N4548	31.04±0.08	Virgo–M87	•	•	•		Graham et al. 1998
N4496A	31.02±0.07	Virgo–N4472		•	•	○	Gibson et al. 2000
N4535	31.10±0.07	Virgo–N4472		•	•		Macri et al. 1999
N4536	30.95±0.07	Virgo–N4472		•	•	•	Gibson et al. 2000
N4639	31.80±0.09	Virgo–N4649		○		•	Gibson et al. 2000
N5253	27.61±0.11	Cen A Group				•	Gibson et al. 2000
N7331	30.89±0.10	N7331 Group	•		•		Hughes et al. 1998

^aCepheid distance modulus (random errors only; the systematic error is 0.16 mag.).

^bGroup/cluster definition is given in Ferrarese et al. 2000b.

^cA bullet identifies galaxies used as calibrators for the method. An open circle defines potential calibrators which are however not used.

^dFull references are given in Ferrarese et al. 2000b.

2. Surface Brightness Fluctuations

The KP calibration of the Surface Brightness Fluctuation method (Tonry & Schneider 1988) is discussed in Ferrarese et al. (2000a). The largest database of SBF measurements comprises ~ 300 galaxies within the local supercluster, observed from the ground in the Kron-Cousins I -band by John Tonry and collaborators (Tonry et al. 1999, Ajhar et al. 2000). A much smaller (~ 20 galaxies), but more distant survey has employed the WFPC2 on board HST (Ajhar et al. 1997, Thomsen et al. 1997, Pahre et al. 1999, Lauer et al. 1998); indeed, it is from this pool of ~ 20 galaxies that the six at $cz \sim 3000 - 7000 \text{ km s}^{-1}$ have been singled out by the KP for deriving H_0 . The use of HST for SBF measurements has some drawbacks, however: the calibration of the fluctuation magnitudes cannot proceed directly against the Cepheids, since only one galaxy, M31, is in common between the two methods. Furthermore, fluctuation magnitudes are known to depend strongly on the metallicity (traditionally expressed as a $V-I$ color) of the underlying stellar population (Tonry et al. 1997). Such a dependence cannot be properly quantified for the HST-SBF sample because of its limited size (Ajhar et al. 1997). Both problems can be overcome, but they certainly are important enough to deserve further study. As for the color dependence, the KP approach is to assume it to be the same as determined empirically for the larger ground based I -band survey (Tonry et al. 1997). This choice is supported by stellar population synthesis models (Worthey 1994), and the similar response curves of the I and the filter used for the HST/WFPC2 measurements, F814W.

Once the color dependence is accounted for, the absolute magnitude of the fluctuations measured with HST can be derived using the 16 galaxies which also have ground based I -band SBF measurements, calibrated against the Cepheids. The latter calibration, however, poses some further problems: all galaxies with I -SBF and Cepheid distances (see Table 1) are early-type spirals, for which SBF measurements become challenging (Tonry et al. 1999). Dust and other contaminants can conspire to artificially brighten the measured fluctuations, and the stellar population in bulges might not be identical to that of the ellipticals which are the preferred targets of the method (leading to a different color dependency). On the other hand, using only SBF data to early-type galaxies would force an indirect calibration whose validity relies on the precarious assumption of a spatial coincidence between late and early-type galaxies, further aggravated by the small sample of galaxies with Cepheid distances in any group. Given the current data (Ferrarese et al. 2000b), the direct calibration for the six galaxies in Table 1, and the indirect one for the six groups/clusters with mean Cepheid and SBF distances (including Leo I, Virgo and Fornax), differ by 0.1 mag, the indirect calibration leading to larger distances. To avoid uncertainties introduced by cluster depth effects, the KP has preferred the direct calibration, but we stress that the reliability of the SBF measurements in spirals remains to be tested, and coupled with the not fully satisfactory constraints imposed on the color dependence of HST-SBF, is the main source of concern in the present calibration of the SBF method.

Because the 5 galaxies comprising the SBF distant sample are confined within 5000 km s^{-1} (excluding the not very well constrained measurement in the Coma cluster by Thomsen et al. 1997), SBF is more susceptible to the effects of large scale flows than the other indicators. Furthermore, three of the five

galaxies lie in the immediate vicinity of one of the major contributors to the local flow field, i.e., the Great Attractor. To provide a first order estimate of the bias introduced by the flow field in estimating H_0 , we considered a simple multi-attractor model fully described in Mould et al. (2000). The model assumes three mass concentrations, the local supercluster, the Great Attractor, and the Shapely Concentration, acting independently so that corrections for each are additive. Using velocities corrected for this flow model, and the HST-SBF distances derived using the direct calibration described above, we obtain $H_0 = 69 \pm 4$ (random) ± 5 (systematic) $\text{km s}^{-1} \text{Mpc}^{-1}$. H_0 happens to remain unaltered if velocities corrected to the CMB frame are used instead; nevertheless, we estimate an $8 \text{ km s}^{-1} \text{Mpc}^{-1}$ random error on H_0 *per cluster* due to corrections for the flow field. This represents the major contributor to the random uncertainty, random errors in the fluctuation magnitudes and $V-I$ colors carry only 30% of the weight. The systematic uncertainty is due mostly to the systematic error in the Cepheid distance scale (the distance to the LMC and the photometric calibration of the WFPC2), and partly to the internal error in the SBF calibration.

3. Fundamental Plane

Among the distance indicators targeted by the KP, the Fundamental Plane (FP) has the distinct disadvantage of not being calibratable directly against the Cepheids. The approach followed for the KP by Kelson et al. (2000) is to base the FP calibration on the Leo I group and the Fornax and Virgo clusters, for which several Cepheid distances exist. Based on Monte Carlo simulations following Gonzales & Faber (1997), Kelson et al. test the hypothesis of a spatial coincidence between the Cepheid spirals and the FP ellipticals in these clusters, and conclude that this assumption leads to an underestimate of the FP distances. Accurate evaluation of this bias would require a detailed knowledge of the clusters' 3D spatial structure which, alas, is lacking. The simulations suggest a 5% downward correction to H_0 , but at the very high price of a 5% uncertainty, which alone will account for a quarter of the systematic error budget on H_0 .

The kinematic data (i.e., the velocity dispersion) used by Kelson et al. for the fundamental plane in Leo I, Virgo and Fornax are from Dressler et al. (1987) and Faber et al. (1989), while the photometric parameters (i.e., effective radius and surface brightness) are derived from original I -band data. The distant sample consists of 11 clusters observed in Gunn r by Jorgensen et al. (1995ab) in the range $cz \sim 1100 - 12000 \text{ km s}^{-1}$. For consistency, the slope of the FP for the calibrators is assumed to be the same as for the distant sample, the I band photometry for the local calibrators is transformed to Gunn r , and the velocity dispersion is corrected to the same aperture used for the distant sample. None of these steps produces major contributions to the error budget.

There appear to be no additional major impediments with the calibration: the zero points derived from the three clusters are consistent with each other. In view of the findings of Fruchter et al. (this volume) it is noteworthy, even if inconsequential, that the FP dispersion is found to be almost double in Fornax compared to Virgo and Leo I (~ 0.09 dex compared to ~ 0.05 dex). The calibration applied to the distant sample leads to $H_0 = 78 \pm 7$ (random) ± 8 (systematic)

km s⁻¹ Mpc⁻¹. The major source of random uncertainty is associated with the slope and zero point of the fundamental plane and only in part with the Cepheid distances of the calibrating clusters. The systematic uncertainty derives mainly from the systematic error in the Cepheid distance scale, the uncertain accounting of the spatial separation between spirals and ellipticals (see above), and only in minor part from cluster population incompleteness bias.

4. Tully-Fisher Relation

The KP calibration of the *BVRIH* Tully-Fisher relations is presented in Sakai et al. (2000). A summary has been written by Shoko Sakai for these proceedings, therefore only a few words will be spent here. The calibration, based on 21 galaxies with Cepheid distances (Table 1), is applied to four distant cluster samples. Of these the largest is the *I*-band survey of Giovanelli et al. (1997), which comprises 555 galaxies in 24 clusters within 9500 km s⁻¹. The *B* and *V*-band samples of Bothun et al. (1985) and the *H*-band sample of Aaronson et al. (1982, 1986) span a comparable range in redshift space, but are of significantly smaller size. The most significant problem with the TF analysis is the discrepancy, at the 2 σ level, between the values of H_0 derived from the *I* and *H* surveys: 74 ± 2 km s⁻¹ Mpc⁻¹ and 67 ± 3 km s⁻¹ Mpc⁻¹ respectively (random errors only). Sakai et al. thoroughly investigated the cause of this discrepancy, and even though a secure culprit could not be identified, circumstantial evidence points to the *H*-band photometry as the most likely suspect. Work is in progress (Macri et al. 2000) to re-derive *H* magnitudes for the local calibrators, and resolve the *I vs H* disagreement. At this time, the most prudent course of action is to adopt a weighted average of the values of H_0 from all four surveys. This leads to $H_0 = 71 \pm 4$ (random) ± 10 (systematic) km s⁻¹ Mpc⁻¹. The random error is shared equally by errors in the CMB velocities for the distant samples, and the random error in the Tully-Fisher moduli (mainly deriving from errors in the photometry, and only partly in the linewidths). The systematic uncertainties come from the systematic error in the Cepheid distance scale and in the TF zero point. Notice that unlike SBF and FP, which target the dust free environments of early-type galaxies, TF and SNIa carry the extra burden of having to deal with internal extinction, which produces an additional term in the final error budget.

5. Type Ia Supernovae

A chronicle on H_0 from Type Ia Supernovae (SNIa) would be divided into three chapters. In chapter 1, values in the upper 50s would be routinely recorded under the assumption that the magnitude at peak acts as a standard candle (Hamuy et al. 1996, Riess et al. 1996, Saha et al. 1997). Chapter 2 opens with the realization that the intrinsic brightness at maximum light correlates with the decline rate (as first suggested by Phillips 1993): slow decliners are intrinsically brighter than fast decliners. Because the local calibrators happen to be slower decliners than the average SNIa in the distant samples, correction for this effect leads to a substantial 8% increase in H_0 (Saha et al. 1999, Hamuy et al. 1996, Riess et al. 1998, Phillips et al. 1999). The KP wrote chapter 3 by re-deriving

Cepheid distances to the local SNIa host galaxies (Gibson et al. 2000), thus revising the calibration and leading to a further 6% increase in H_0 .

It is thanks to the effort of Allan Sandage and collaborators if we can now rely on Cepheid distances to six nearby SNIa host galaxies when none existed before (Saha et al. 1994, 1995, 1996a, 1996b, 1997, 1999), even if nothing compares to the strategic planning of Tanvir et al. (1995) who published a Cepheid distance to NGC 3368 three years before its SNIa went off. Loyal to the KP commitment of providing a consistent footing to all secondary distance indicators, Gibson et al. (2000) set out to derive new photometry and distances to all of the SNIa host galaxies. In two cases (NGC 4496A and IC4182) the new distances agree with the ones originally published; but in all other cases the re-analysis led to consistently smaller distance moduli, by an average of 0.12 magnitudes. The causes of the discrepancies vary from galaxy to galaxy; they include disagreement in the photometry (which are quickly amplified by the dereddening procedure used in deriving the distance moduli), differences in the sample of Cepheids, and differences in the treatment of reddening. Many pages of justifications and details are given in Gibson et al.; the punch line is that these new distances should be preferred when SNIa are compared to the other secondary distance indicators, as they are derived in a consistent manner as for the 18 galaxies originally observed as part of the KP.

Three local supernovae are excluded from the calibration because of the poor quality of their light curves: SN1895B in NGC 5253 (the galaxy also hosted the better sampled SN1972E) and the SNe in NGC 4414 and NGC 4496A. Gibson et al. follow Suntzeff et al. (1999) in the adoption of the SNe data (B , V and I photometry and extinction corrections) for both the local and distant sample. The latter comprises 35 Calán-Tololo/CfA SNe (Phillips et al. 1999), in the range $cz \sim 1000 - 31000 \text{ km s}^{-1}$. Both the distant and nearby samples are corrected for the decline rate versus peak luminosity relation obtained by Phillips et al. (1999) from a low extinction subset of the Calán-Tololo SNe. Averaging the B , V and I data Gibson et al. derive a weighted Hubble constant of $H_0 = 68 \pm 2$ (random) ± 5 (systematic) $\text{km s}^{-1} \text{ Mpc}^{-1}$. The main contributions to the random errors come from the scatter in the Hubble diagram and from errors in the photometry and distances for the local calibrators. The systematic error is propagated directly from the Cepheid distance scale.

How does the KP value of H_0 compare to the findings of other groups? We will consider the two most recent works. Suntzeff et al. (1999), which is the source of the KP database for both the local and distant SNe, quote $H_0 = 63 \pm 2 \text{ km s}^{-1} \text{ Mpc}^{-1}$ which, as expected, agrees with Gibson et al. when the new distances for the local calibrators are accounted for. Saha et al. (1999) obtain $H_0 = 60 \pm 2 \text{ km s}^{-1} \text{ Mpc}^{-1}$ in both B and V . Part of the difference with Gibson et al. is again due to the adoption of new distances, but an additional 6% must be accounted for. This is due to differences in the internal extinction corrections for the local sample, and in the foreground extinction for the distant sample (the two having opposite effects on H_0), and in the actual photometry adopted for the local SNe. Other factors, such as the adoption of slightly different distant samples, different formalism for the rate of decline versus peak magnitude relation, and different assumption as to a dependence of H_0 on redshift, do not produce appreciable differences.

6. Combining the Constraints

By combining the constraints imposed on H_0 by each indicator (Figure 2), we can reduce the propagation of uncorrelated systematics. There is some amount of covariance in the values of H_0 from Table 2, due for example to the sharing of some of the calibrator galaxies (Table 1), and to the common underlying assumption on the distance to the LMC. To properly account for the interplay of random and systematic errors, Mould et al. (2000) have developed Monte Carlo simulations in which all uncertainties and parameter dependences for each indicator are propagated through and investigated thoroughly. **The final result is $H_0=71\pm6$ km s⁻¹ Mpc⁻¹. The error distribution is symmetrical, with a 1σ width of 9%, fulfilling the KP original goal.**

Table 2. H_0 from Secondary Distance Indicators

Indicator	σ^a	No. ^b	No. ^b	Δv^c	H_0^d	Systematics ^e		
SBF	0.11	6	4	3900–4700	69±4±6	1% ↑	5% ↓	N/A
FP	0.045	16	11	1100–12000	78±7±8	1% ↑	6% ↓	2%
TF	0.19	21	24	1000–11500	71±4±10	1% ↑	4% ↓	2%
SNIa	0.14	6	35	1000–31000	68±2±5	2% ↑	4% ↓	N/A
Combined					71±6	1% ↑	5% ↓	

^aThe intrinsic dispersion for each indicator, in magnitudes for TF, SBF and SNIa, and dex for FP.

^bThe number of local calibrators and of clusters/galaxies in the distant sample respectively.

^cVelocity range (in km s⁻¹) spanned by the distant sample.

^dIn km s⁻¹ Mpc⁻¹. The errors listed are random and systematic, in this order

^eSystematic change in H_0 resulting from (in order) corrections for the local flow field, a dependence of the distance moduli on Cepheid metallicity as in Kennicutt et al. (1998), and population incompleteness bias in the distant sample.

7. Future Directions

There is still substantial room for improvement in the result given above. One common dimension they all share is the assumption of a 50 ± 3 kpc distance to the LMC. A distribution of LMC distances compiled from the literature (Mould et al. 2000), if indeed peaked at 50 kpc, is not symmetric: red clump distances are as low as 43 kpc (e.g., Stanek et al. 1999), while Mira variables define the upper envelope at 55 kpc (Reid 1998). Mould et al. investigate the consequences of replacing the adopted probability distribution with this empirical, skewed compilation. As a result H_0 would increase by 4.5%, and the associated error would jump to 12%. While this is an extreme, and somewhat unorthodox revision, it does illustrate the rather heavy repercussion of this one assumption. The debate on the LMC distance promises to be as heated as the controversy on H_0 itself, and a resolution might have to await the launch of SIM in 2005. In the meantime, an update on the LMC PL relation is long overdue: the current calibration is based on 32 Cepheids, less than the Cepheid sample size of several KP galaxies! Progress is being made (e.g., Moffett 1998, Barnes et al. 1999, Tanvir & Boyle 1999, Udalski et al. 1999); within the KP, Kim Sebo is leading an effort which has so far produced *BVRIH* light curves for over 200 LMC Cepheids (Sebo et al. 2000). Finally, systematics in the calibration of the PL relation must also be explored in more galaxies having Cepheid-independent distance estimates:

promising starts are the study conducted by Maoz et al. (1999) in NGC 4258, and the DIRECT project targeting M31 and M33 (e.g., Mochejska et al. 1999).

The metallicity dependence of the Cepheid PL relation, and the uncertainties in the photometric calibration of the WFPC2, closely follow the LMC distance in generating the largest uncertainty in H_0 . While the latter will soon be better constrained (Stetson et al. 2000, Saha et al. 2000), not much agreement has yet been reached for the former (e.g., Alibert et al. 1999, Caputo et al. 1999, Storm et al. 1998, Sasselov et al. 1997, Kochanek 1997). If the mild, and only marginally significant, metallicity dependence found for the KP by Kennicutt et al. (1998) is applied to the Cepheid distances of the local calibrators, the value of H_0 would decrease by 4.5%.

Further progress is also to be expected in improving the calibrator samples for some of the secondary distance indicators. Sandage and collaborators are still actively hunting down SNIa hosts. Indeed in the near future three more calibrators will be added to the current sample of six. One is a member of Fornax, and will help to better constrain the distance to the cluster needed for the FP calibration. Finally, during this conference we learned that a lot of effort is being spent in developing new distant samples (Germany, Willick, Courteau, Giovanelli, Colless, this volume). In particular, the Mount Stromlo Abell Cluster SN Search (see also Reiss et al. 1998) coupled with the ongoing Calán-Tololo and Asiago surveys, promises to double the current number of distant SNe, with the result that not only the Hubble diagram, but also dependences of the peak magnitude on second parameters can be further refined. The *I*-band Tully-Fisher sample of Dale et al. (1999) will push the method to 25000 km s⁻¹, twice as far as the sample currently used by the KP, while Fundamental Plane parameters for 80 new clusters are expected from the EFAR project.

References

- Aaronson, M., et al. 1982, ApJS, 50, 241
- Aaronson, M., et al. 1986, ApJ, 302, 536
- Ajhar, E. A., et al. 1997, AJ, 114, 626
- Alibert, Y., et al. 1999, A&A, 344, 551
- Barnes, T., et al. 1999, astro-ph/9903095
- Bothun, G. D., et al. 1985, ApJS, 57, 423
- Caputo, F., et al. 1999, astro-ph/9902279
- Cardelli, J. A., et al. 1989, ApJ, 345,245
- Dale, A. D., et al. 1999, astro-ph/9907059
- Dressler, A., et al. 1987, ApJ, 313, 42
- Faber, S. M., et al. 1989, ApJS, 69, 763
- Ferrarese, L., et al. 2000a, ApJ, in press (astro-ph/9908192)
- Ferrarese, L., et al. 2000b, ApJS, submitted
- Freedman, W. L., et al. 2000, in preparation
- Gibson, B., et al. 2000, ApJ, in press (astro-ph/9908149)
- Giovanelli, R., et al. 1997, AJ, 113, 22
- Gonzales, A. H., & Faber, S. M. 1997, ApJ, 485, 80
- Hamuy, M., et al. 1996, AJ, 112, 2398
- Huchra, J., & Mader, J. 1998, <http://cfa-www.harvard.edu/~huchra>, ZCAT Version July 15, 1998
- Jorgensen, I., et al. 1995a, MNRAS, 273, 1097
- Jorgensen, I., et al. 1995b, MNRAS, 276, 1341
- Kelson, D., et al. 2000, ApJ, submitted
- Kennicutt, R. et al. 1998, ApJ, 498, 181
- Kochanek, C. S. 1997, ApJ, 491, 13
- Lauer, T. R., et al. 1998, ApJ, 499, 577
- Macri, L., et al. 2000, ApJS, submitted
- Madore, B. F. & Freedman, W. L. 1991, PASP, 103, 933
- Maoz, E. et al. 1999, Nature, in press, astro-ph/9908140
- Mochejska, B. J., et al. 1999, astro-ph/9904343
- Moffett, T. J., et al. 1998, ApJS, 117, 135
- Mould, J. R., et al. 2000, ApJ, submitted
- Pahre, M. A., et al. 1999, ApJ, 515, 79
- Phillips, M. M. 1993, ApJ, 413, 105
- Phillips, M. M., et al. 1999, astro-ph/9907052
- Reid, I. N. 1998, AJ, 115, 204
- Reiss, D. J., et al. 1998, AJ, 115, 26
- Riess, A. G., et al. 1996, ApJ, 473, 88
- Riess, A. G., et al. 1998, AJ, 116, 1009
- Saha, A., et al. 1994, ApJ, 425, 14
- Saha, A., et al. 1995, ApJ, 438, 8
- Saha, A., et al. 1996a, ApJ, 466, 55
- Saha, A., et al. 1996b, ApJS, 107, 693
- Saha, A., et al. 1997, ApJ, 486, 1
- Saha, A., et al. 1999, astro-ph/9904389
- Sakai, S., et al. 2000, ApJ, submitted
- Sasselov, D., et al. 1997, A&A, 324, 471
- Stanek, K. Z., et al. 1999, astro-ph/9908041
- Storm, J., et al. 1998, astro-ph/9811376
- Suntzeff, N., et al. 1999, AJ, 117, 1175
- Tanvir, N. R., & Boyle, A. 1999, MNRAS, 304, 957
- Tanvir, N. R. et al. 1995, Nature, 377, 27
- Thomsen, B., et al. 1997, ApJ, 483, L37
- Tonry, J. L., & Schneider, P. 1988, AJ, 96, 807
- Tonry, J.L, et al. 1997, ApJ, 475, 399
- Tonry, J. L., et al. 1999, astro-ph/9907062
- Udalski, A., et al. 1999, astro-ph/9907236
- Willick, J. A. 1999, ApJ, 516, 47
- Worthey, G. 1994, ApJS, 95, 107

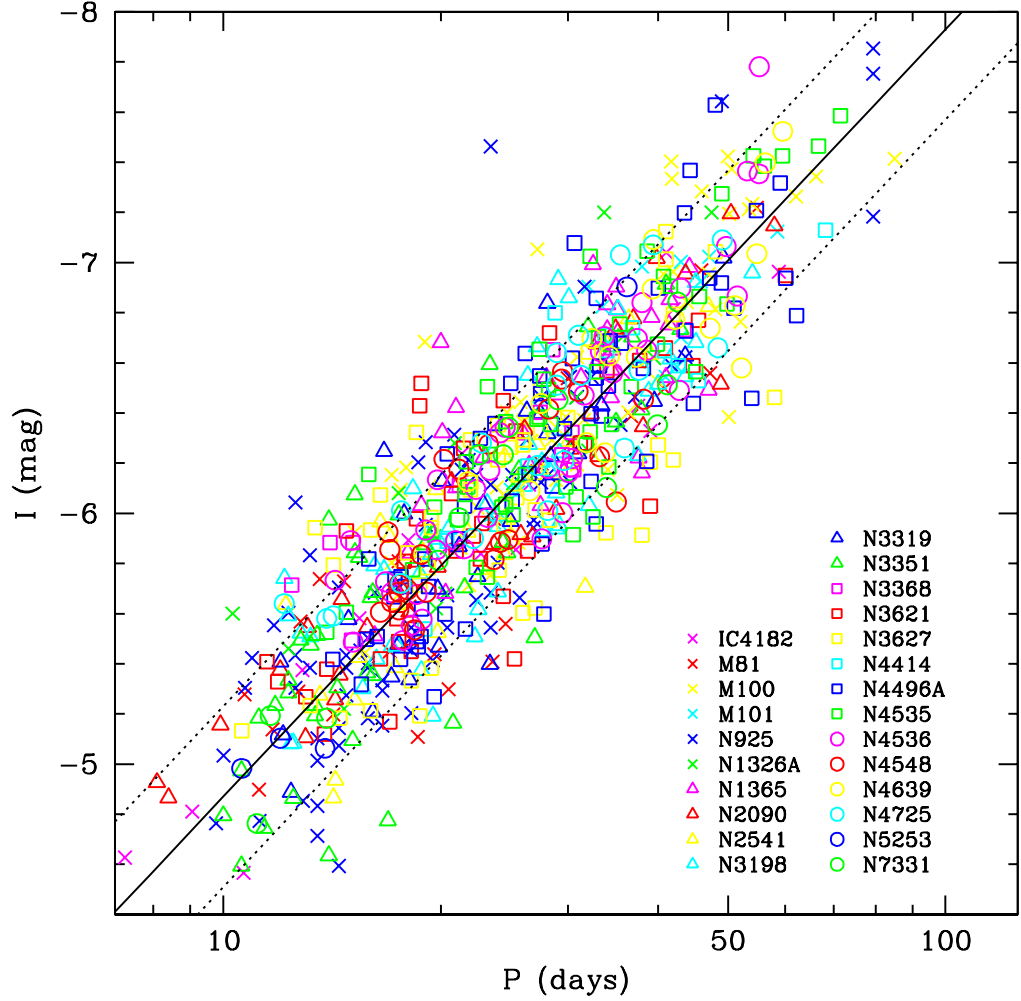


Figure 1. A composite I -band PL relation showing all Cepheids discovered as part of the Key Project and other HST efforts (references in Table 1). The count is just shy of 800 objects. Apparent magnitudes are converted to absolute magnitudes using the distances in Table 1, and the reddening derived for each galaxy. The solid line represents the calibrating LMC PL relation, and the dotted lines its 2σ uncertainty, deriving from the finite width of the instability strip.

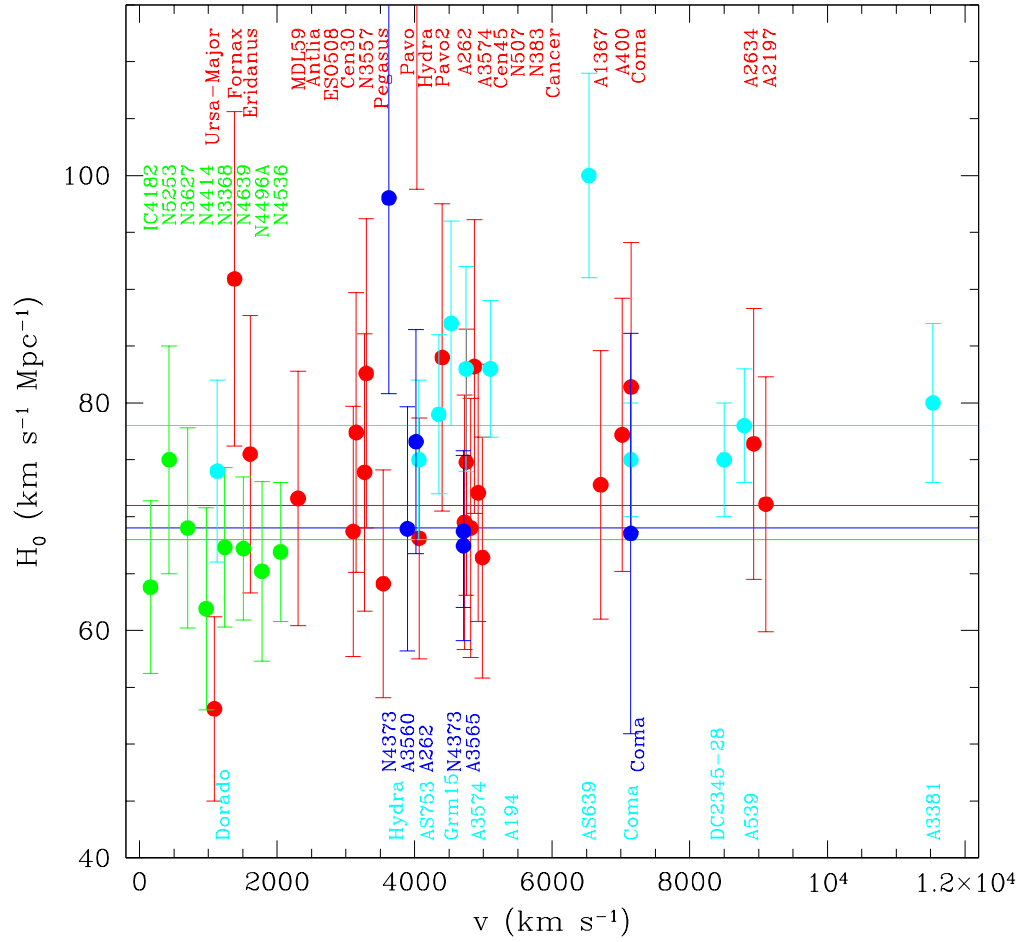


Figure 2. H_0 derived from the distant cluster sample for Tully-Fisher (red), SBF (blue), and Fundamental Plane (cyan). For SNIa (green) we plot the values of H_0 given by each of the local calibrators when applied to the Hubble diagram produced by the distant sample of Phillips et al. (1999). Velocities are CMB velocities for Tully-Fisher, SBF and Fundamental Plane, heliocentric velocities for the SNIa calibrators.